Intense Reactivity in Sulfur-Hydrogen Mixtures at High Pressure under X-ray Irradiation

Intense Reactivity in Sulfur-Hydrogen Mixtures at High Pressure under X-ray Irradiation

Edward J. Pace,[†] Amy L. Coleman,[‡] Rachel J. Husband,[¶] Huijeong Hwang,[§] Jinhyuk Choi,[§] Taehyun Kim,[§] Gilchan Hwang,[§] Sae Hwan Chun,[‖] Daewoong Nam,[‖] Sangsoo Kim,[‖] Orianna B. Ball,[†] Hanns-Peter Liermann,[¶] Malcolm I. McMahon,[†] Yongjae Lee,[§,⊥] and R. Stewart McWilliams*[,†]

[1]

†*SUPA, School of Physics and Astronomy & Centre for Science at Extreme Conditions, The University of Edinburgh, Edinburgh EH9 3FD, United Kingdom*

‡*Lawrence Livermore National Laboratory, 7000 East Avenue, Livermore, California, 94500, USA*

¶*Photon Sciences, Deutsches Elektronen-Synchrotron (DESY), Hamburg, Germany*

§*Institute for High-Pressure Mineral Physics & Chemistry, Yonsei University, Seoul, Republic of Korea*

‖*Pohang Accelerator Laboratory, Pohang, Gyeongbuk 37673, Republic of Korea*

⊥*Center for High Pressure Science & Technology Advanced Research, Shanghai 201203, China*

E-mail: rs.mcwilliams@ed.ac.uk

Abstract

Superconductivity near room-temperature in the sulfur-hydrogen system arises from a sequence of reactions at high pressures, with x-ray diffraction experiments playing a central role in understanding these chemical-structural transformations and the corresponding S:H stoichiometry. Here we document x-ray irradiation acting as both a probe and as a driver of chemical reaction in this dense hydride system. We observe reaction between molecular hydrogen (H_2) and elemental sulfur (S_8) under high pressure, induced directly by x-ray illumination, at photon energies of 12 keV using a free electron laser. The rapid synthesis of hydrogen sulfide (H_2S) at 0.3 GPa was confirmed by optical observations, spectroscopic measurements, and micro-structural changes detected by x-ray diffraction. These results document x-ray induced chemical synthesis of superconductor-forming dense hydrides, revealing an alternative production strategy and confirming the disruptive nature of x-ray exposure in studies on high-pressure hydrogen chalcogenides, from water to high-temperature superconductors.

Graphical TOC Entry

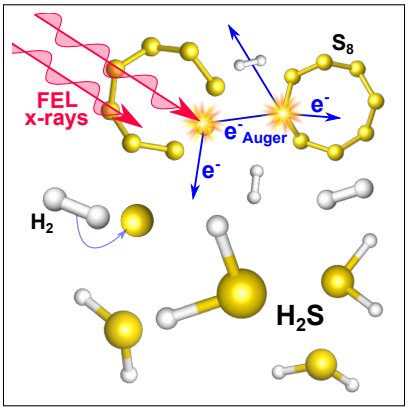

The behavior of simple hydrides under extreme conditions is of fundamental importance to achieving superconductivity at high temperatures,[1–6] with chemical bonds between hydrogen atoms (H) and heavier elements favoring high phonon frequencies. Recently, the high-pressure formation of H_2S (and H_2Se) from constituent elements has been of substantial interest, following early predictions[7,8] and then observation of a high superconducting transition temperature (T_c) of 203 K in the S-H system at pressures above 155 GPa,[2,9–13] with similar properties predicted in the analogous selenium-hydrogen (Se-H) system.[14,15] The experimentally observed high T_c in the hydrogen-sulfur system is considered to occur in H_3S, a high-pressure phase containing a high content of hydrogen.[2,8,16,17] H_3S (T_c = 204 K) is predicted to form above 111 GPa from the reaction between H_2 and H_2S, upon compression of the stoichiometrically equivalent, molecular van-der-Waals compound $(H_2S)_2H_2$.[8,18] This compound (and structurally analogous $(H_2Se)_2H_2$) itself forms above 4 GPa upon room-temperature compression of H_2 and H_2S (H_2Se).[11–13,18] Formation of the initial H_2 and H_2S (H_2Se) mixtures is facilitated by directly reacting the constituent elements S (Se) and excess H_2 at high pressures within diamond anvil cells, a sluggish process near room temperature.[11–13]

Hard x-ray experimental probes, in particular x-ray diffraction (XRD), have been crucial in the characterization of the structures, reactions, stoichiometries and high-pressure phase transformations of S-H and Se-H systems.[9,10,12,16,18,19] However, there are notable inconsistencies in the results of the XRD studies within both the S-H[9,10,16] and Se-H[12,13] systems, though the reasons for these differences are currently unclear.

In fact, x-ray exposure itself is observed to cause material changes within the electronically analogous oxygen-hydrogen (O-H) system, where irradiation of H_2O by hard x-rays of intermediate energy ($\sim$10 keV) induces a chemical transformation to an O_2-H_2 alloy.[20,21] This raises the prospect that x-ray exposure could have a chemical effect on other chalcogen (group 16 element) hydride systems under pressure, yet this question remains unexplored. Additionally, the effect of the x-ray source intensity on reaction rates must be explored: while prolonged synchrotron x-ray irradiation of the O-H system induced a reaction over several hours (order 10^3 s),[20] the high inten-

sity of modern sources such as x-ray free electron lasers (XFELs) may induce more rapid reactions. This may be an essential consideration when taking advantage of the high-brilliance of x-ray pulses from XFEL sources, such as for high-resolution diffraction[22–24] and chemical dynamics[25] studies that are not possible at synchrotrons. XFELs have been demonstrated to be advantageous for the study of very high pressure conditions, thus far using dynamic compression methods,[22–24] but have not yet been used in conjunction with static compression techniques.

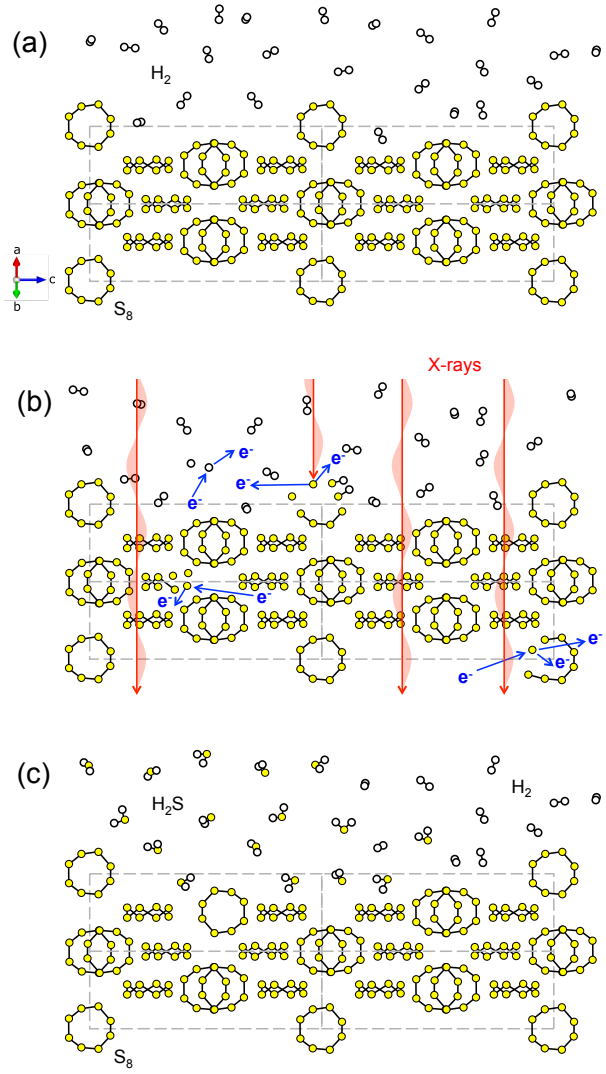

Figure 1: Chemical reactivity induced by XFEL exposure under high pressure. An initial crystalline (orthorhombic) sulfur sample (2 unit cells shown, viewed diagonally between the *a* and *b* axes) adjacent to fluid hydrogen compressed to 0.3 GPa (a) is exposed to a burst of hard x-rays from a free electron laser (b), causing photoelectron and secondary electron damage across the sample disrupting 1-10% of S_8 molecules, leading to rapid etching of the sulfur and formation of phase separated H_2S just after the exposure (c).

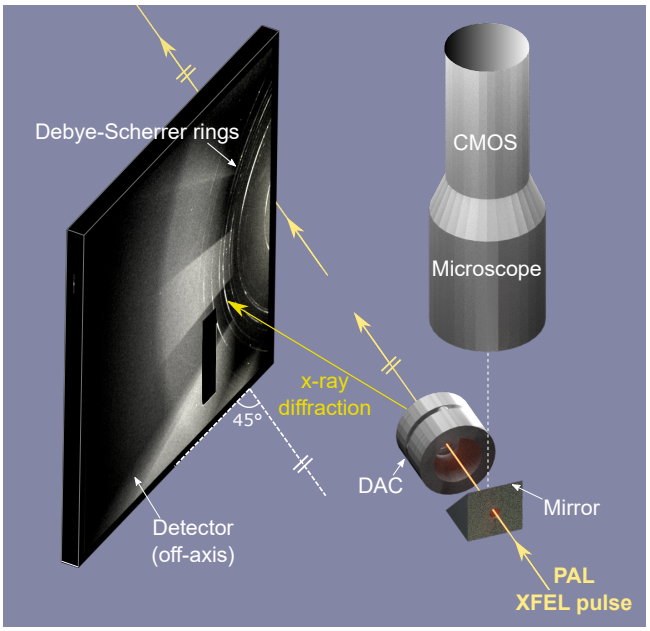

Figure 2: Representation of the experimental set-up used at the XSS beamline of the X-ray Free Electron Laser at the Pohang Accelerator Laboratory (PAL-XFEL).[26,27] The beam is directed horizontally through the axis of the diamond-anvil-cell (DAC). The diffraction detector is placed behind and to the side of the sample at ∼45° to the incident direction of the x-ray beam, to avoid damage from direct contact. The microscope provides *in situ* microscopy of the sample chamber viewed along the DAC axis using an angled mirror, via which the beam is transmitted through a small hole.

Here we present the results of XFEL irradiation of S and H_2 under static compression, and demonstrate an unambiguous high-pressure chemical reaction that is induced (Fig. 1), and probed, by the femtosecond (10^{-15} s) x-ray exposures. The experimental configuration is shown in Figure 2 and described in detail in the Supporting Methods. A diamond anvil cell (DAC) was prepared with pieces of crystalline sulfur surrounded by fluid hydrogen at 0.3 GPa. XFEL pulses were passed through the sample cavity, diffracting from the solid portions of the sample. The x-ray intensity was gradually increased; higher powers were sufficient to initiate a visible, rapid reaction between S and H_2, and alter the diffraction patterns indicating physical changes in the sulfur component. The short duration of each pulse means that any physical changes to the sample induced by a given XFEL pulse are observed in the diffraction pattern produced by the following pulse.[28]

The diffraction patterns showed that the orthorhombic S_8 (α) phase persisted from shot to shot (Fig. 3). However, above a given x-ray power, the Debye-Scherrer ring azimuthal intensity

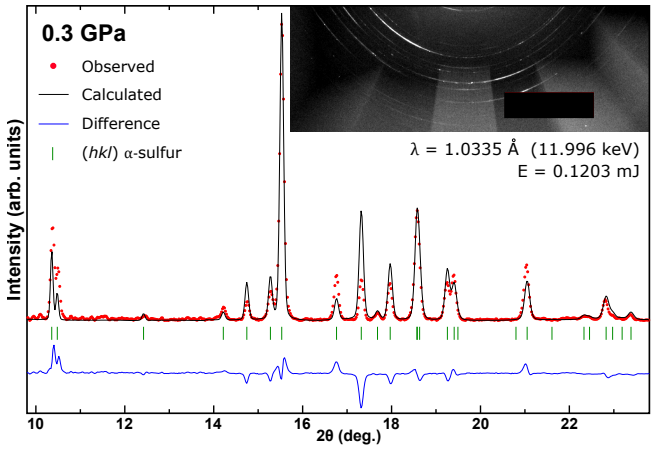

Figure 3: Rietveld refinement of the orthorhombic α-S structure to the integrated profile obtained from the sum of the four diffraction images shown in Figure 4, showing the observed (points) and calculated (line) diffraction patterns, the calculated reflection positions (vertical lines), and the difference profile (lower line). The four 2D diffraction images were summed to help reduce the effects of sample texture. The refined parameters for space group $Fddd$ are a = 10.380(3) Å, b = 12.770(1) Å, and c = 24.421(3) Å (density of 2.105 g cm^{-3}); see Supporting Methods for further details.

distributions shifted, evidencing microstructural changes in sulfur. The most pronounced changes were observed at the highest tested power (Fig. 4). The visual appearance of the solid S_8 also changed coincident with the pulses (Fig. 5). Over the duration of the experiment, the initially precompressed translucent flake became a scattered powder at the irradiation point (Fig. 5b).

Immediately upon exposure of the sample to the XFEL pulse, we observed a small vesicle forming at the point of irradiation, which moved steadily downward through the fluid hydrogen medium, before disappearing upon reaching the edge of the sample chamber (see Supplementary Video). This was interpreted as a rapidly-produced bubble of the reaction product H_2S, the stable hydride of S at these pressures. The motion is consistent with a dense H_2S vesicle (1.03 g cm^{-3})[29] sinking through the lower density molecular hydrogen medium (0.10 g cm^{-3}),[30] where isothermal equations of state are used as heat associated with the reaction should dissipate within milliseconds,[31] before the bubble moves. Following Stokes law for a spherical particle falling through a fluid,[32] the velocity v is related to the medium viscosity μ, particle radius R, and densities of the

particle (ρ_p) and medium (ρ_m), as

$$v = \frac{2gR^2(\rho_p - \rho_m)}{9\mu}\gamma \tag{1}$$

where γ is a correction factor, of order 0.1-1.0, that depends on the nature of the motion and proximity to a wall (diamond culet). With a measured bubble velocity of $\sim$160 μm/s and diameter of $\sim$8 μm, and considering the viscosity of hydrogen[30] ($\mu = 2.8 \times 10^{-5}$ Pa s), the bubble's motion is consistent with a fall of a pure H_2S vesicle immediately adjacent to the culet ($\gamma \sim 0.1$),[32] as would be expected for a reaction occurring in the vicinity of the S_8 flake attached to the culet.

Raman analysis before and after the XFEL exposures confirmed that a chemical reaction between S_8 and H_2 had been induced, from the appearance of the characteristic fluid H_2S stretching mode at 2610 cm^{-1} (Fig. 5a).[33,34] The H_2S signal was ubiquitous throughout the fluid H_2 region of the sample, indicating that the concentration was low enough for the phases to be mixed (ratio of H_2S:$H_2 \ll 1$), as at higher concentrations ($\sim$ 1:1) H_2S and H_2 separate into distinct fluid regions.[12,18] In contrast, the appearance of a small bubble of the product immediately after the reaction is attributed to temporary phase separation made possible by an intense localized reaction, that quickly enhanced the local concentration of product before dissolution could proceed. Treating the bubble as pure H_2S, and assuming it comprises all or most of the product from a single x-ray pulse, the product mass is estimated as 2.8×10^{-13} kg per pulse. Given the x-ray beam diameter of 14 μm, this implies that the volume of solid S_8 which reacts as a result of each x-ray pulse is equivalent to a $\sim$ 0.8 μm thickness of the solid S_8 layer in the area of the beam, accounting for its elevated density under pressure (Fig. 3). The initial S_8 layer thickness is $\sim$15 μm, therefore about 5% of the exposed S_8 is reacted with each exposure. This explains the disintegration of the S_8 flake (Fig. 5b) in the region of irradiation after $\sim$17 pulses above the detectable reaction threshold.

These observations collectively indicate that an intense chemical reaction between S_8 and H_2 is induced by x-ray illumination on the femtosecond timescale. In contrast, at room temperature without x-ray excitation there is no evidence of H_2S formation from samples of S_8 in fluid H_2 at

similar pressures on a timescale of two weeks (the time between loading and final observation in this study). Synthesis of H_2S from S_8 and H_2 was therefore attributed exclusively to exposure to x-ray photons.

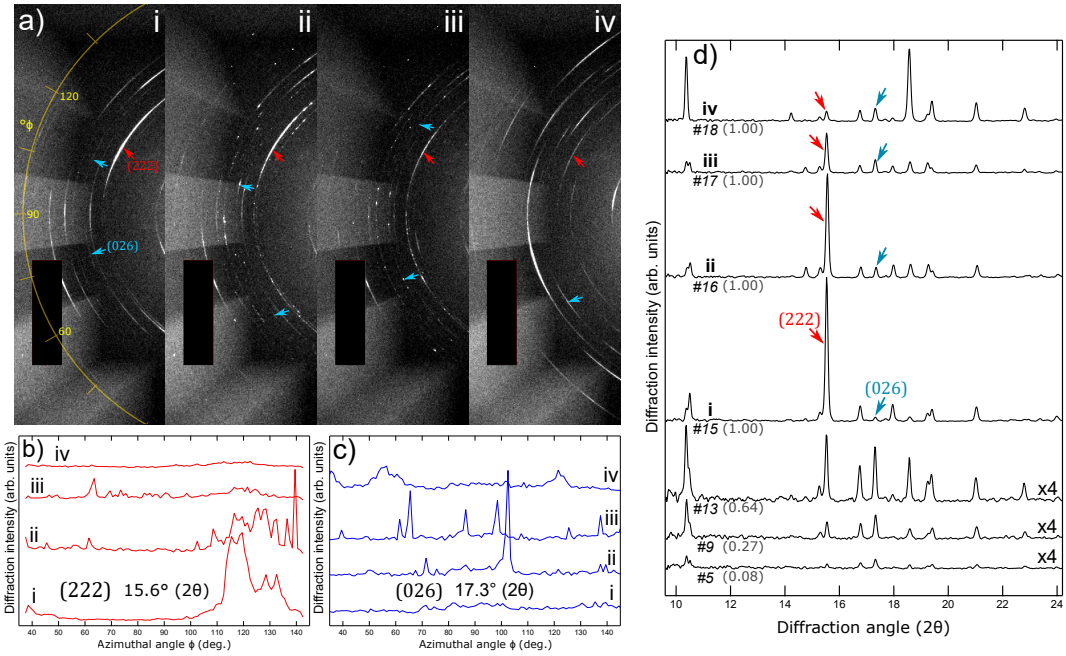

Figure 4: The microstructure changes induced by XFEL exposure. a) Detector images showing the textured Debye-Scherrer rings arising from S_8 upon four successive exposures to XFEL pulses at the highest pulse energy used in this experiment (0.120 mJ/pulse). All four images were obtained from the region of the sample indicated in Fig. 5b, and were obtained at $\sim$1 s intervals. Each diffraction image shows the state of the sample produced by the previous XFEL pulse. The azimuthal angle ϕ is shown in yellow in (i), and the black rectangular areas in the images cover an area of damage to the detector. Plots b) and c) show the azimuthal variations in the intensity of the (222) (red) and (026) (blue) Debye-Scherrer rings (identified in (a) by the red and blue arrows), respectively, in each of the four images. The changes in intensity distribution arise from the texture changes induced by each XFEL pulse. d) Azimuthally integrated S diffraction patterns as a function of increasing XFEL energy. Each pattern is labelled by shot number (#) followed by fraction of maximum pulse energy in brackets. The intensities of the three patterns obtained at lower pulse energies are scaled up by a factor of four; the patterns obtained at maximum pulse energy are integrated profiles of 4a) i - iv.

The absorption of an x-ray pulse by the sample initially disrupts the electrons, while the atoms remain fixed in place. The energy absorbed in the sample per volume (H) is estimated as

$$H = \Lambda\alpha \tag{2}$$

where Λ is the x-ray beam energy density within the sample, and α is the local absorption coefficient, i.e. of either the sulfur or hydrogen component. The number of x-ray absorption events in the sample, per volume, is H/E_{ph}, where E_{ph} is the photon energy (12 keV). Considering the number of atoms in the same volume, the number of absorption events in hydrogen is very low, or about one event per 10^9 atoms at peak power, whereas for S_8 there is one absorption event for every $\sim 10^5$ atoms; we thus concentrate on the S_8 component. If we also account for electron-impact ionization cascades (affecting a further $10^2 - 10^3$ atoms[28]), and the disruption of one S_8 molecule of α-S per ionization (Fig. 1), we can expect a direct electronic disruption of bonding for roughly 1-10% of S atoms following each x-ray pulse. The dominant process will thus involve ionization of atoms by electron collisions, with core electron expulsion and subsequent Auger decay rapidly ionising and fragmenting the S_8 rings (e.g. $S_8 \rightarrow S + S_7^{2+} + 2e^-$). The disrupted S could then rapidly react with adjacent, or plausibly interstitial, molecular hydrogen in an attempt to fill valence p-orbitals; unstable ring-fragments could break down further in similar interactions. We do not see any evidence, from Raman and XRD measurements, of other allotropes of sulfur forming; therefore the S_8 rings must break down completely or re-form. The fraction of irradiated S atoms directly affected by x-ray energy deposition and ionization is similar to that consumed by the reaction in a single pulse, estimated on the basis of optical observations to be of order 5%. Therefore, it is plausible that the intense reaction observed is driven primarily by the chemical disruption of the sample during and immediately after the femtosecond irradiation, which then undergoes a rapid reaction to form H_2S.

Previous evidence of photochemistry in both S-H and Se-H systems has been identified from the partial formation of H_2S (H_2Se) upon prolonged exposure to laser light of sufficient energy (2.3 eV) and substantial flux.[11,13] Our study shows a considerably more intense and complete photoreaction between S and H_2 resulting from the delivery of a large dose of keV energy photons. In such a photochemical process, the total dose of radiation can be critical in driving a reaction. A similar process may thus occur under lower power (i.e. synchrotron) hard x-ray irradiation on longer but routinely accessed timescales. Indeed, photochemically driven molecular reorganization was reported in the H-O system using synchrotron x-rays of comparable photon energy over a much

longer period.[20] While these qualitative comparisons suggest that the total dose and the photon energy are critical parameters, nonlinear effects of high beam intensity including multiple ionization, bulk chemical disruption, and sample heating may also be enhancing the reaction intensity.

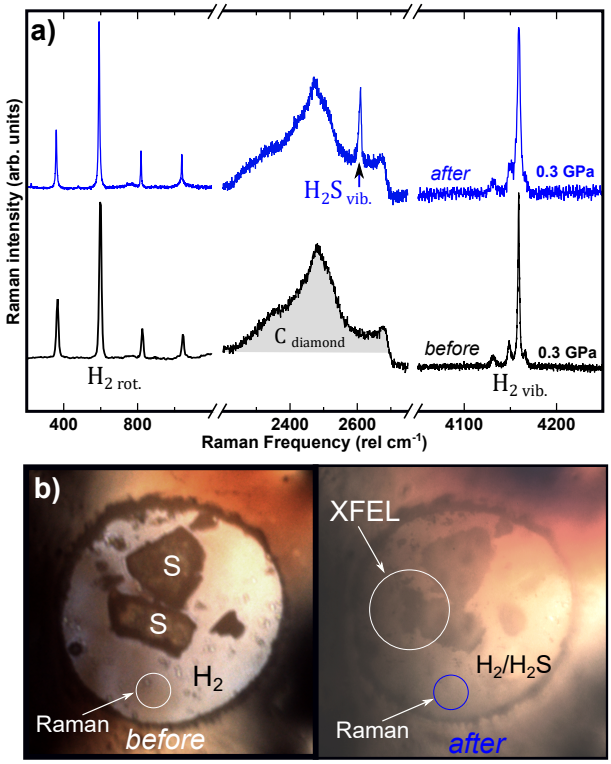

Figure 5: a) Raman spectra obtained within H_2 media before (black) and after (blue) exposure to high intensity x-rays. The black spectrum shows pure H_2 whilst the blue spectrum shows a mixture of H_2S dissolved in fluid H_2. b) photomicrographs of the DAC sample chamber before and after x-ray exposure. The position of the Raman laser-spot is indicated on both images; the right image shows the area exposed to XFEL pulses.

Concomitant with electronic chemical disruption is the rapid thermalization of the hot electrons on a timescale of $\sim 10^{-12}$ seconds,[28,31] leading to an equilibrium heated state in S_8 (direct heating of H_2 is negligible). This hot state in the S_8 persists on timescales of $\sim 10^{-6}$ seconds before quenching and will additionally heat the surrounding hydrogen to high temperatures.[31] Temperature induced reaction and subsequent formation of hydrides under pressure is well documented, for example as a result of laser-heating S in H_2,[9,10,19] and gentle heating of Se in H_2 at 473 K.[12] The equilibrium peak temperature (before heat dissipation) in these experiments can be estimated

as[31]

$$T - T_0 = \frac{H}{\rho C_P} \tag{3}$$

where ρ is the density and C_P the heat capacity at constant pressure of the sample. The temperature achieved in S_8 during the pulse is thus estimated to peak at $\sim$1000 K. As similarly elevated temperatures can themselves enhance a chemical reaction between S and H_2, it is possible that this contributes partially to the total reaction progression, but as the heating timescale is extremely short compared to existing studies,[9,10,19] this may not have as strong an effect as the direct electronic disruption.

It is worth observing that such a peak temperature is well in excess of the melting point of solid S under pressure (477 K at 0.3 GPa[35]). Therefore, the successive changes to the microstructure of the crystalline S_8 (Fig. 4) must be related both to the sample breakup associated with the reaction (Fig. 5b), and also to the local melt and recrystallization of bulk S, as these processes occur well before the arrival of the subsequent x-ray pulse and diffraction measurement. In particular, the change in the texture of the Debye-Scherrer rings from smooth arcs (Fig 4a.i), to spotty points of intensity (Fig 4a.ii-iii), then back to smooth arcs (Fig 4a.iv) is suggestive of both crystallite displacement and melt recrystallization. In summary, we find that the reaction mechanism is one where the XFEL pulse induces flash localized heating and massive chemical disruption in the S, some of which reacts with adjacent or interstitial H_2 thus forming H_2S, while unreacted molten S recrystallizes back into orthorhombic α-S_8.

In conclusion, we find that an intense high-pressure chemical reaction between sulfur and hydrogen can be initiated by hard x-ray pulses from a free electron laser. Delivery of a large x-ray photon dose (10^{11} photons) in a short time (fs) produces rapid chemical damage as well as sample heating, primarily localized to the higher-Z reactant (crystalline S). This reactivity in the S-H system, induced by the x-rays, shows interesting differences from those in the high-pressure O-H system,[20] with formation rather than dissociation of hydride phases. This suggests a potentially rich x-ray induced reaction behavior in chalcogen hydride systems at high pressures. This important observation is relevant to high pressure experiments concerning the superconducting S-H

system, where the reaction behavior and results of x-ray experiments have been in dispute.[9,10,16]

Our study shows that x-ray irradiation at high photon energies may not act simply as a non-invasive probe of the structural and molecular state of this system, as is commonly assumed, but may in fact cause reactivity that would otherwise not be observed. These effects must be further investigated as functions of pressure, in both S-H and Se-H systems, and may also provide a novel synthesis route in superconductor forming hydrides.

Our study finally benchmarks a new application for XFEL radiation in high-pressure chemistry studies under static compression, demonstrating a strategy for non-destructive XFEL probing and excitation using robust sample confinement in a diamond anvil cell, and the ability to obtain high-quality diffraction data from such samples in femtoseconds. With new experimental regimes expected to be accessible with advances in capabilities at 4^{th} generation x-ray sources, such as improved brilliance and faster pulse-repetition rates, it is important to gain a comprehensive understanding of their effect on high pressure materials systems in order to fully take advantage of these modern light sources.

Acknowledgements

The X-ray experiment was performed at the beamline XSS (proposal no. 2019-1st-XSS-018) at PAL-XFEL funded by the MSIP. We acknowledge Vitali Prakapenka, Sang-Heon Dan Shim, Leora Dresselhaus-Cooper, Hyunchae Cynn, Toshimori Sekine, Hae Ja Lee and Eric Galtier for fruitful discussions, Clemens Prescher for assistance with analysis, and Hyojung Hyun for beamline assistance. YL thanks the support by the Leader Researcher program (NRF-2018R1A3B1052042) of the Korean Ministry of Science, ICT and Planning (MSIP). EJP and MIM acknowledge support from EPSRC Grant EP/R02927X/1, and RSM from EPSRC Grant EP/P024513/1. We acknowledge DESY (Hamburg, Germany), a member of the Helmholtz Association HGF, for the provision of experimental facilities. Parts of this research were carried out in collaboration with PETRA III. The work by ALC was performed under the auspices of the U.S. Department of Energy by

Lawrence Livermore National Laboratory under Contract No. DE-AC52-07NA27344.

Supporting Information Available: Supporting methods and supplementary video recording.

References

(1) Ashcroft, N. W. Hydrogen dominant metallic alloys: high temperature superconductors?. *Phys. Rev. Lett.* **2004**, *92*, 187002.

(2) Drozdov, A. P.; Eremets, M. I.; Troyan, I. A.; Ksenofontov, V.; Shylin, S. I. Conventional superconductivity at 203 kelvin at high pressures in the sulfur hydride system. *Nature* **2015**, *525*, 73–76.

(3) Liu, H.; Naumov, I. I.; Hoffmann, R.; Ashcroft, N. W.; Hemley, R. J. Potential high-T_c superconducting lanthanum and yttrium hydrides at high pressure. *Proc. Natl. Acad. Sci. U. S. A.* **2017**, *114*, 6990–6995.

(4) Peng, F.; Sun, Y.; Pickard, C. J.; Needs, R. J.; Wu, Q.; Ma, Y. Hydrogen clathrate structures in rare earth hydrides at high pressures: possible route to room-temperature superconductivity. *Phys. Rev. Lett.* **2017**, *119*, 107001.

(5) Somayazulu, M.; Ahart, M.; Mishra, A. K.; Geballe, Z. M.; Baldini, M.; Meng, Y.; Struzhkin, V. V.; Hemley, R. J. Evidence for superconductivity above 260 K in lanthanum superhydride at megabar pressures. *Phys. Rev. Lett.* **2019**, *122*, 027001.

(6) Drozdov, A. P.; Kong, P. P.; Minkov, V. S.; Besedin, S. P.; Kuzovnikov, M. A.; Mozaffari, S.; Balicas, L.; Balakirev, F. F.; Graf, D. E.; Prakapenka, V. B. et al. Superconductivity at 250 K in lanthanum hydride under high pressures. 2019.

(7) Li, Y.; Hao, J.; Liu, H.; Li, Y.; Ma, Y. The metallization and superconductivity of dense hydrogen sulfide. *The Journal of Chemical Physics* **2014**, *140*, 174712.

(8) Duan, D.; Liu, Y.; Tian, F.; Li, D.; Huang, X.; Zhao, Z.; Yu, H.; Liu, B.; Tian, W.; Cui, T. Pressure-induced metallization of dense $(H_2S)_2H_2$ with high-T_c superconductivity. *Sci. Rep.* **2014**, *4*, 6968.

(9) Goncharov, A. F.; Lobanov, S. S.; Prakapenka, V. B.; Greenberg, E. Stable high-pressure phases in the H-S system determined by chemically reacting hydrogen and sulfur. *Phys. Rev. B* **2017**, *95*, 140101.

(10) Guigue, B.; Marizy, A.; Loubeyre, P. Direct synthesis of pure H_3S from S and H elements: No evidence of the cubic superconducting phase up to 160 GPa. *Phys. Rev. B* **2017**, *95*, 020104(R).

(11) Duwal, S.; Yoo, C.-S. Reversible photochemical transformation of S and H_2 Mixture to $(H_2S)_2H_2$ at High Pressures. *J. Phys. Chem. C* **2017**, *121*, 12863–12870.

(12) Pace, E. J.; Binns, J.; Peña Alvarez, M.; Dalladay-Simpson, P.; Gregoryanz, E.; Howie, R. T. Synthesis and stability of hydrogen selenide compounds at high pressure. *J. Chem. Phys.* **2017**, *147*, 184303.

(13) Zhang, X.; Xu, W.; Wang, Y.; Jiang, S.; Gorelli, F. A.; Greenberg, E.; Prakapenka, V. B.; Goncharov, A. F. Synthesis and properties of selenium trihydride at high pressures. *Phys. Rev. B* **2018**, *97*, 064107.

(14) Zhang, S.; Wang, Y.; Zhang, J.; Liu, H.; Zhong, X.; Song, H.-F.; Yang, G.; Zhang, L.; Ma, Y. Phase diagram and high-temperature superconductivity of compressed selenium hydrides. *Sci. Rep.* **2015**, *5*, 15433.

(15) Flores-Livas, J. A.; Sanna, A.; Gross, E. K. U. High temperature superconductivity in sulfur and selenium hydrides at high pressure. *Eur. Phys. J. B* **2015**, *89*, 63.

(16) Einaga, M.; Sakata, M.; Ishikawa, T.; Shimizu, K.; Eremets, M. I.; Drozdov, A. P.;

Troyan, I. a.; Hirao, N.; Ohishi, Y. Crystal structure of the superconducting phase of sulfur hydride. *Nat. Phys.* **2016**, *12*, 835–839.

(17) Errea, I.; Calandra, M.; Pickard, C. J.; Nelson, J. R.; Needs, R. J.; Li, Y.; Liu, H.; Zhang, Y.; Ma, Y.; Mauri, F. Quantum hydrogen-bond symmetrization in the superconducting hydrogen sulfide system. *Nature* **2016**, *532*, 81–84.

(18) Strobel, T. A.; Ganesh, P.; Somayazulu, M.; Kent, P. R. C.; Hemley, R. J. Novel cooperative interactions and structural ordering in H_2S-H_2. *Phys. Rev. Lett.* **2011**, *107*, 255503.

(19) Goncharov, A. F.; Lobanov, S. S.; Kruglov, I.; Zhao, X.-M.; Chen, X.-J.; Oganov, A. R.; Konôpková, Z.; Prakapenka, V. B. Hydrogen sulfide at high pressure: change in stoichiometry. *Phys. Rev. B* **2016**, *93*, 174105.

(20) Mao, W. L.; Mao, H.-K.; Meng, Y.; Eng, P. J.; Hu, M. Y.; Chow, P.; Cai, Y. Q.; Shu, J.; Hemley, R. J. X-ray–induced dissociation of H_2O and formation of an O_2–H_2 alloy at high pressure. *Science* **2006**, *314*, 636–638.

(21) Fukui, H.; Hiraoka, N.; Hirao, N.; Aoki, K.; Akahama, Y. Suppression of X-ray-induced dissociation of H_2O molecules in dense ice under pressure. *Scientific Reports* **2016**, *6*, 26641.

(22) Briggs, R.; Gorman, M. G.; Coleman, A. L.; McWilliams, R. S.; McBride, E. E.; McGonegle, D.; Wark, J. S.; Peacock, L.; Rothman, S.; Macleod, S. G. et al. *Phys. Rev. Lett.* 025501.

(23) Gorman, M. G.; Coleman, A. L.; Briggs, R.; McWilliams, R. S.; Hermann, A.; McGonegle, D.; Bolme, C. A.; Gleason, A. E.; Galtier, E.; Lee, H. J. et al. Recovery of metastable dense Bi synthesized by shock compression. *App. Phys. Lett.* **2019**, *114*, 120601.

(24) Coleman, A. L.; Gorman, M. G.; Briggs, R.; McWilliams, R. S.; McGonegle, D.; Bolme, C. A.; Gleason, A. E.; Fratanduono, D. E.; Smith, R. F.; Galtier, E. et al. Identification of phase transitions and metastability in dynamically compressed antimony using ultrafast x-ray diffraction. *Phys. Rev. Lett.* **2019**, *122*, 255704.

(25) Minitti, M. P.; Budarz, J. M.; Kirrander, A.; Robinson, J. S.; Ratner, D.; Lane, T. J.; Zhu, D.; Glownia, J. M.; Kozina, M.; Lemke, H. T. et al. Imaging molecular motion: femtosecond x-ray scattering of an electrocyclic chemical reaction. *Phys. Rev. Lett.* **2015**, *114*, 25501.

(26) Kang, H. S.; Min, C. K.; Heo, H.; Kim, C.; Yang, H.; Kim, G.; Nam, I.; Baek, S. Y.; Choi, H. J.; Mun, G. et al. Hard X-ray free-electron laser with femtosecond-scale timing jitter. *Nat. Photon.* **2017**, *11*, 708–713.

(27) Park, J.; Eom, I.; Kang, T. H.; Rah, S.; Nam, K. H.; Park, J.; Kim, S.; Kwon, S.; Park, S. H.; Kim, K. S. et al. Design of a hard x-ray beamline and end-station for pump and probe experiments at Pohang Accelerator Laboratory X-ray Free Electron Laser facility. *Nucl. Instrum. Methods Phys. Res. A* **2016**, *810*, 74–79.

(28) Nass, K. Radiation damage in protein crystallography at X-ray free-electron lasers. *Acta Cryst. D* **2019**, *75*, 211–218.

(29) Ihmels, E. C.; Gmehling, J. Densities of toluene, carbon dioxide, carbonyl sulfide, and hydrogen sulfide over a wide temperature and pressure range in the sub- and supercritical state. *Ind. Eng. Chem. Res.* **2001**, *40*, 4470–4477.

(30) Michels, A.; Schipper, A. C.; Rintoul, W. H. The viscosity of hydrogen and deuterium at pressures up to 2000 atmospheres. *Physica* **1953**, *19*, 1011–1028.

(31) Meza-Galvez, J.; Gomez-Perez, N.; Marshall, A.; Coleman, A. L.; Appel, K.; Liermann, H. P.; Konopkova, Z.; McMahon, M. I.; McWilliams, R. S. *arXiv*: Thermomechanical response of thickly tamped targets and diamond anvil cells under pulsed hard x-ray irradiation. **2018**, 1806.10893.

(32) King, H. E.; Herbolzheimer, E.; Cook, R. L. The diamond-anvil cell as a high-pressure viscometer. *J. App. Phys.* **1992**, *71*, 2071–2081.

(33) Anderson, A. I.; Demoor, S.; Hanson, R. C. Raman study of a new high pressure phase of hydrogen sulfide. *Chem. Phys. Lett.* **1987**, *140*, 471–475.

(34) Shimizu, H.; Nakamichi, Y.; Sasaki, S. Pressure-induced phase transition in solid hydrogen sulfide at 11 GPa. *J. Chem. Phys.* **1991**, *95*, 2036.

(35) Vezzoli, G. C.; Dachille, F.; Roy, R. Melting curve of sulfur to 31 kilobars. *Inorg. Chem.* **1969**, *8*, 2658–2661.